International Journal of Heat and Technology
Vol. 41, No. 6, December, 2023, pp. 1397-1406
Journal homepage: http://iieta.org/journals/ijht

Optimization of Heat Transfer in Solar-Powered Biodiesel Reactors Using Alumina Nanofluids: A Combined Experimental and Numerical Study

Mustafa M. Hathal[1,2*], Osama A. Mohsen[2,3], Hasan Sh Majdi[2,4], Basim O. Hasan[2,5]

[1] Chemical Engineering and Material Science Doctoral School, University of Pannonia, Veszprém 8200, Hungary
[2] Scientific Society for Energy Studies and Research, Baghdad 10011, Iraq
[3] Chemical and Petrochemical Engineering Department, University of Anbar, Anbar 31002, Iraq
[4] Chemical Engineering and Petroleum Industry Department, Al-Mustaqbal University, Hilla 51001, Iraq
[5] Chemical Engineering Department, Al-Nahrain University, Baghdad 10011, Iraq

Corresponding Author Email: mus.mhathal@gmail.com

https://doi.org/10.18280/ijht.410601

Received: 5 July 2023
Revised: 6 August 2023
Accepted: 14 August 2023
Available online: 31 December 2023

Keywords:
biodiesel thermal reactor, solar system, nanofluid, computational fluid dynamics (CFD)

ABSTRACT

The challenge posed by waste cooking oil (WCO) accumulation in sewage systems necessitates innovative solutions. This study presents an investigation into enhancing biodiesel production from WCO by augmenting heat absorption using oil-alumina nanofluids in a plug flow reactor powered by photovoltaic (PV) solar cells. Nanofluids with varying alumina concentrations (0%, 0.1%, 0.5%, and 2%) were examined. The investigation comprised two phases: Initially, nanoparticles were visualized via transmission electron microscopy (TEM), followed by the determination of nanofluid physical properties, including thermal conductivity, density, viscosity, and heat capacity. Subsequently, these properties were integrated into a finite element method (FEM) numerical simulation of the solar reactor using COMSOL Multiphysics. The study further involved design of experiments, regression analysis, and optimization techniques to elucidate the relationship between absorbed heat (Qc), oil flow rate (q), and nanoparticle volume percent (fi). The results indicate that an oil flow rate (q) of 0.0000173 m^3/s and a nanoparticle volume percent (fi) of 2% significantly enhance heat absorption by approximately 43%. This research not only addresses the accumulation of WCO in sewage systems but also proposes a novel method to reduce fouling by utilizing biodiesel production. The findings underscore the efficiency of oil-alumina nanofluids in a plug flow solar reactor and the impact of varying nanoparticle concentrations on heat absorption. The physical properties of the nanofluid and its performance in the solar reactor are meticulously documented. Furthermore, the study delineates optimal operational conditions, resulting in a substantial increase in heat absorption. These insights are instrumental in developing sustainable waste oil management strategies and leveraging renewable energy sources within sewage systems.

1. INTRODUCTION

The imperative of reducing greenhouse gas emissions is paramount in confronting climate change and its extensive repercussions on society, encompassing economic, political, biodiversity, food security, environmental quality, and public health dimensions. A 2020 report by the World Health Organization (WHO) revealed that emissions linked to climate change are responsible for approximately 4.2 million deaths annually. Renewable energy sources are integral in mitigating these emissions, as they lessen the dependency on fossil fuels. These fuels are significant contributors to greenhouse gas emissions, primarily through combustion in thermal power plants and internal combustion engines. Since 1990, solar PV energy has been the most prevalently adopted renewable energy source, catering to both residential and industrial electricity demands [1]. PV cells are characterized by their versatility, integration capability with existing power networks and non-renewable thermal power plants, adaptability across various operational scales, and the potential to stabilize and regulate power through integration features [2].

A critical issue in the domain of photovoltaic cells is the rise in cell temperature, which leads to increased electrical resistance and a consequent reduction in power output. It has been recognized in prior research that this temperature escalation results from the power generation process and the excess heat flow due to PV cells' inefficiency [3]. Consequently, cooling PV panels is essential to optimize solar cell power. Earlier studies have underscored the feasibility of utilizing the generated heat in various applications, such as energy storage, water heating systems, and building heat pumps [4-7]. Notably, the maximum heat flow aligns with the peak power output at noon, albeit with a diminished power efficiency, resulting in a 33% efficiency decrease as reported in source 5. Neglecting to harness this generated heat not only

leads to the forfeiture of electrical energy but also contributes to an elevated ambient atmosphere within buildings. This escalation poses challenges to HVAC systems, especially during summer months [8].

Previous research has extensively investigated nanoparticles for their potential to augment heat absorption and enhance heat transfer characteristics. Kumar et al. [9] conducted a detailed review of the performance improvement of photovoltaic modules via nanofluid cooling. The study underscored the enhanced heat transfer coefficient attained by integrating nanoparticles into the bulk fluid, resulting in superior heat absorption and transfer capabilities.

Further research, such as the work of Albadr et al. [10], Xuan and Li [11], and Senthilraja and Vijayakumar [12], has delved into the heat transfer attributes of nanofluids, including the utilization of Al_2O_3 nanoparticles. These investigations have collectively illustrated an increase in thermal conductivity by approximately 60% when nanoparticles are present. Additionally, Gupta et al. [13] reviewed the heat transfer mechanisms in heat pipes employing nanofluids, emphasizing the extensive interfacial area produced by nanoparticles and the influence of dynamic mechanisms on the enhancement of heat transfer.

Mangrulkar et al. [14] and Buongiorno and Hu [15] undertook experimental investigations into convective heat transfer enhancement using alumina/water and copper oxide/water nanofluids, respectively. Their results affirmed the capacity of nanofluids to ameliorate heat transfer properties. Focusing on solar thermal applications, Sekhar et al. [16] studied heat transfer enhancement in a pipe using Al_2O_3 nanofluids and twisted tapes. Bianco et al. [17] discussed heat transfer augmentation with nanofluids, while Mohsen et al. [18] and Khaled and Vafai [19] examined the control of thermal dispersion effects and heat transfer enhancement via different fin geometries. These investigations contribute significantly to understanding the mechanisms underpinning heat transfer improvements in nanofluids. The impact of diverse factors on heat absorption and transfer in nanofluids has been the subject of numerous studies. Sivashanmugam [20] offered a comprehensive overview of nanofluid applications in heat transfer. Borate et al. [21] and Zamzamian et al. [22] explored variations in heat transfer coefficients with differing nanofluid concentrations and flow configurations. Hussein et al. [23] investigated the forced convection nanofluid heat transfer in automotive cooling systems. Liu et al. [24] focused on the thermal conductivities of various nanofluids and their application in water chiller systems. Majdi et al. [25] analyzed the enhancement of heat transfer using aluminum oxide nanofluid on smooth and finned surfaces under turbulent flow. Sundar and Singh [26] reviewed convective heat transfer and friction factor correlations in nanofluids in tubes and with inserts.

The issue of WCO and its repercussions on plumbing systems have been explored in preceding studies. Phan and Phan [27] focused on biodiesel production from waste cooking oils, whereas Degfie et al. [28] optimized biodiesel production using a calcium oxide nanocatalyst. Sahar et al. [29] emphasized an efficient technique for converting waste cooking oil into biodiesel. Zhang et al. [30] discussed the application of solar renewable energy in hydrogen generation, storage, and utilization. Despite considerable research on nanofluids and heat transfer enhancement, the specific investigation into the application of oil-alumina nanofluids for heat absorption in solar photovoltaic cells has been limited.

The aim of this study is to develop and characterize an oil-alumina nanofluid and explore its potential application in augmenting heat transfer and absorption in solar photovoltaic cells. This research primarily seeks to address the challenges associated with the increasing temperatures of solar panels, leading to diminished power output. By integrating nanoparticles, the study endeavors to enhance heat absorption, thereby mitigating excess heat and ultimately elevating the energy efficiency of photovoltaic cells.

The novelty of this study is anchored in the development and characterization of an oil-alumina nanofluid tailored for heat absorption in solar photovoltaic cells. While previous research has extensively explored the use of nanofluids across various domains, a gap remains in their specific application within the realm of solar photovoltaic technology. This research aims to bridge this gap by investigating the capacity of nanoparticles to boost heat transfer and absorption in solar cells. To realize these objectives, the study adopts a design of experiment methodology, employing the advanced statistical software MINITAB 18 for discerning factor interactions. Through rigorous experimentation and data analysis, the study aspires to enhance the performance of a solar-powered biodiesel reactor using the formulated nanofluid. This research's contribution lies in its potential to elevate the energy efficiency of photovoltaic cells via the absorption of heat from sustainable sources. The application of nanoparticles in enhancing heat transfer and absorption presents a novel approach in renewable energy technologies. The outcomes of this study will significantly enrich the existing body of knowledge on nanofluids and their applications, offering invaluable insights for future research and development in renewable energy. This study stands to provide a significant advancement in the field, particularly in terms of applying nanotechnology to improve the functionality and efficiency of renewable energy systems.

2. EXPERIMENTAL DETAILS

2.1 Experimental part procedure

In this study, the investigation focused on enhancing heat transfer and absorption by adding nanoparticles to edible sunflower oil (waste cooking oil after filtration for 6 hours). The nanoparticles selected for this experiment were Alumina gamma nanoparticles. The concentration range of nanoparticles investigated varied from 0-2%. To achieve a homogeneous solution, the nanoparticles were mixed with the oil using a lab-scale mixer (homogenizer). This mixing process ensured proper dispersion of the nanoparticles within the oil. Subsequently, the nanofluid was subjected to ultrasonic treatment using a 750 W and 25000 Hz ultrasonic probe. The ultrasonic treatment played a vital role in forming a stable nanofluid solution, as depicted in Figure 1. The experimental work is elaborated in Al-Mustaqbal University Laboratories.

To visualize the nanofluid and observe the nanoparticles and nano clusters, transmission electron microscopy (TEM) was employed. TEM analysis was conducted at two scales: 20 nm and 0.2 micrometers, revealing the distribution and morphology of the nanoparticles and nano clusters. Figure 2 presents the resulting images. To characterize the thermal and hydrodynamic properties of the nanofluid, several measurements were performed. Heat capacity and thermal

conductivity were measured using a Differential Scanning Calorimeter (DSC). The density of the nanofluid was determined using a hydrometer. Additionally, viscosity measurements were carried out using an electronic viscometer, considering various temperatures and concentrations of nanoparticles. The experiments also involved measuring the incident solar radiation using a radiation meter. This measurement was important to assess the solar radiation during the experimental procedures.

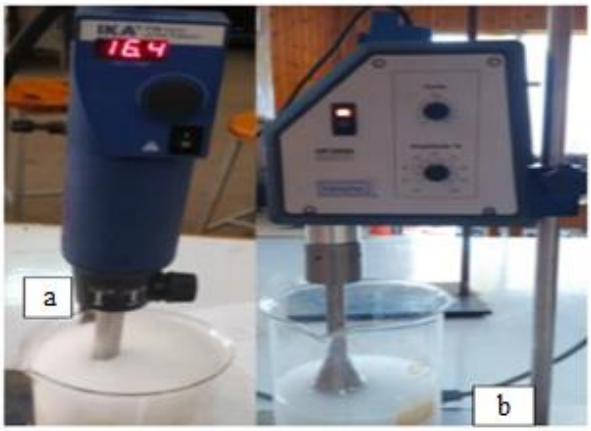

Figure 1. (a) homogenizer, (b) ultrasonic generator

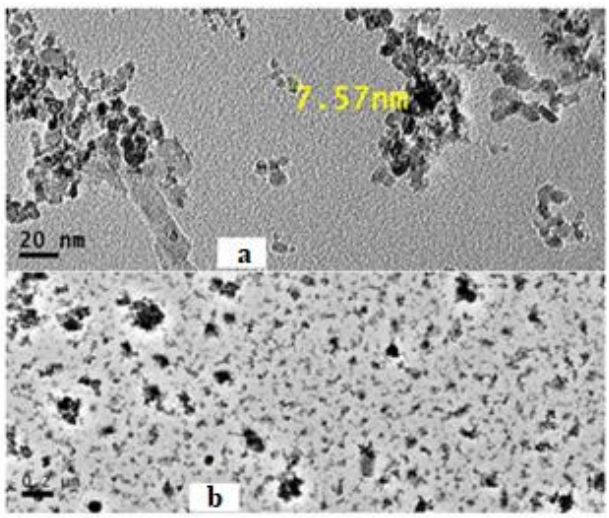

Figure 2. TEM visualizing of oil-alumina nanoparticles: (a) 20 nm, (b) 200 nm

2.2 Experimental results

These experimental findings contribute to the understanding of the thermal properties, density, viscosity, and solar radiation characteristics of the developed oil-alumina nanofluid. The observed trends and relationships provide insights into the performance of the solar-powered biodiesel reactor. The enhanced thermal properties, such as heat capacity and thermal conductivity, offer potential improvements in heat absorption and transfer efficiency. Moreover, the knowledge gained from the density and viscosity measurements can inform the design and optimization of the system, considering factors like mass flow rate, pressure drop, and long-term heat absorption capability. These findings contribute to the broader literature on nanofluids and their applications in renewable energy technologies, offering valuable insights for further research and development in this field.

Figure 3 presents the relationship between heat capacity and temperature for different nanoparticle concentrations (fi). It is observed that as fi increases, the heat capacity decreases. However, when the temperature is increased, the heat capacity rises. The results indicate that the maximum heat capacity is achieved at a temperature of 50°C and a nanoparticle volume fraction (fi) of 0%. It is worth noting that the heat capacity of nanoparticles is generally lower than that of the continuous phase.

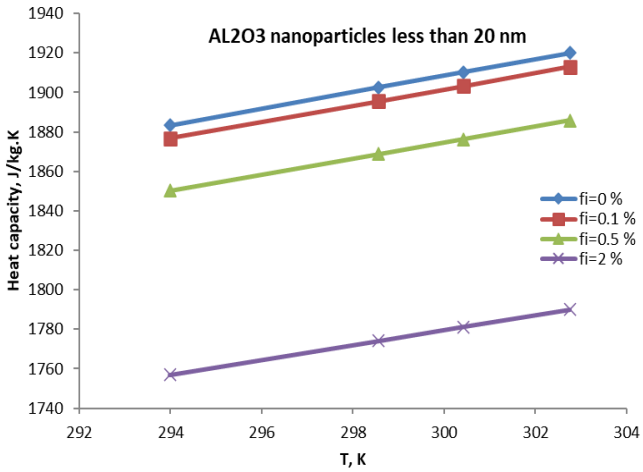

Figure 3. The influence of T and fi on heat capacity

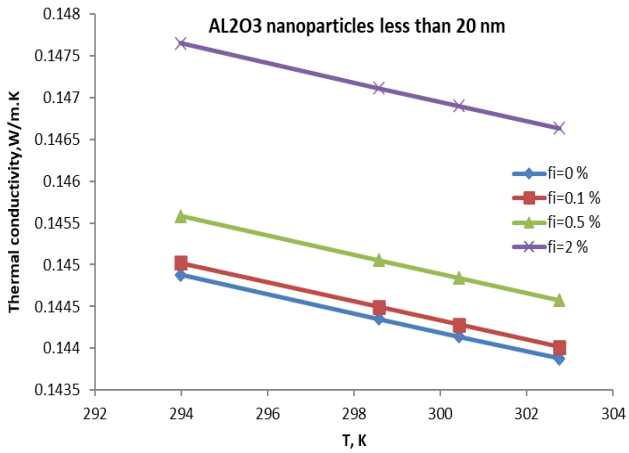

Figure 4. The influence of T and fi on thermal conductivity

Figure 4 illustrates the relationship between temperature and thermal conductivity for various fi values. As the temperature increases, there is a corresponding increase in thermal conductivity, which also applies to different fi values. The higher concentration of nanoparticles leads to an increase in the thermal conductivity of the nanofluid. This can be attributed to the higher thermal conductivity of nanoparticles compared to the continuous phase. However, the scanning electron micrograph in Figure 2 reveals the presence of nano clusters, suggesting the influence of the dynamic mechanism driven by Brownian motion. The kinetic energy of the nanoparticles induced by Brownian motion contributes to the formation of nano clusters. These observations indicate that both the stationary and dynamic mechanisms play a role in enhancing thermal conductivity.

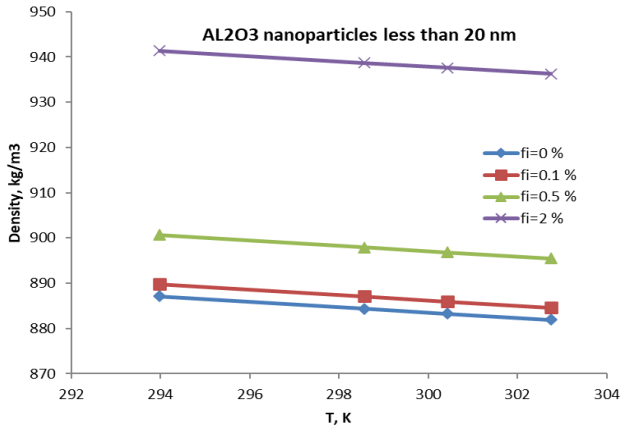

Figure 5. The influence of T and fi on density

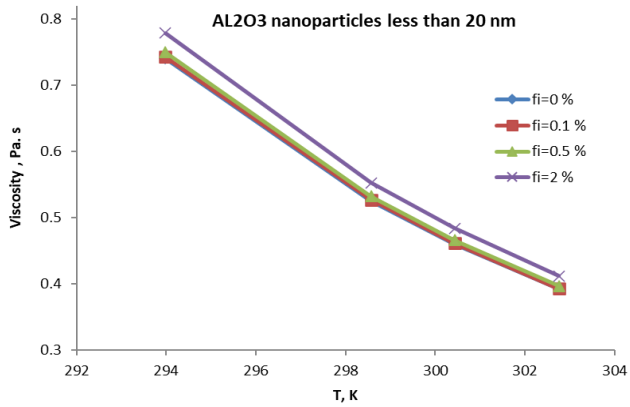

Figure 6. The influence of T and fi on viscosity

Figures 5 and 6 demonstrate the effects of temperature and nanoparticle concentration on density and viscosity, respectively. As the nanoparticle concentration (fi) increases, both density and viscosity proportionally increase, and vice versa. Higher density results in a higher mass flow rate and greater heat absorption capacity. Meanwhile, higher viscosity leads to increased pressure drop, which affects pump efficiency and the formation of fouling layers. These factors have significant implications for the long-term heat absorption performance. The experimental investigation examined the behavior of physical properties, including density, viscosity, thermal conductivity, and heat capacity, in an oil-alumina nanofluid. The study aimed to understand how these properties change with variations in temperature and nanoparticle concentrations. The findings contribute to the broader understanding of nanofluids and their potential applications in renewable energy technologies. The results revealed that nanoparticle concentration plays a crucial role in determining the density and viscosity of the nanofluid. As the concentration of nanoparticles increased, both density and viscosity exhibited proportional increases [19]. These observations have implications for the mass flow rate, heat absorption capacity, and efficiency of the system. Higher nanoparticle concentrations result in higher density, leading to increased mass flow rate and heat absorption. Similarly, increased viscosity affects pump efficiency and can result in the formation of fouling layers over time. The study also investigated the relationship between temperature and thermal conductivity. It was observed that thermal conductivity increased with rising temperatures, as well as with increasing nanoparticle concentrations [17]. The higher thermal conductivity of the nanofluid, attributed to the presence of nanoparticles with superior thermal conductivity compared to the continuous phase, offers potential benefits for enhancing heat transfer and absorption. The formation of nano clusters, driven by Brownian motion, further amplifies the thermal conductivity enhancement [30-33]. In Figure 7, the measured solar radiation is shown as a function of time for various summer months in the Baghdad region during 2020. The solar radiation exhibits an exponential increase from early morning until it reaches an optimal level at 1:00 pm, after which it remains relatively constant. Among the summer months, July shows the highest solar radiation values.

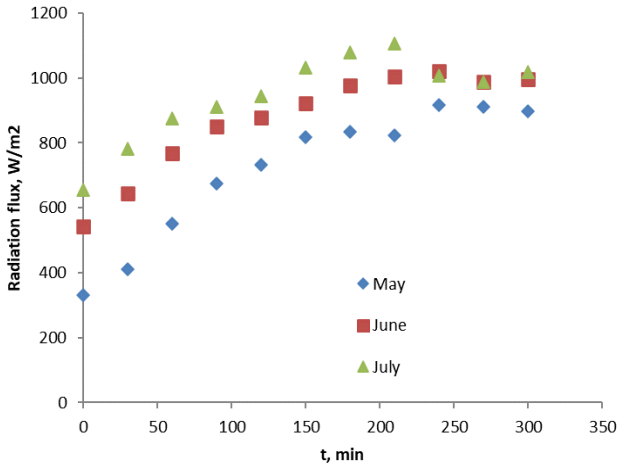

Figure 7. Radiation flux vs. time for various summer months during 2020 in Baghdad region

3. NUMERICAL INVESTIGATION

3.1 Numerical methodology

The heat transfer system was designed to optimize the utilization of the surface area of a silicon panel, incorporating an internal distinct pipe geometry. The meshing process generated a total of 622,476 elements, including vortices, tetrahedra, pyramids, quads, prisms, triangles, edge elements, and vortex elements. These elements were distributed throughout the system, forming a mesh that covered a total area of 0.1351 m^2. The quality of the mesh, which indicates the level of refinement and accuracy, was determined to be 0.00065, as shown in Figure 8. This meshing configuration allows for detailed computational analysis and simulation of heat transfer processes within the system. By utilizing this mesh, the system's geometry is accurately represented, enabling the evaluation of various physical properties and the simulation of heat transfer phenomena. The precise representation of the geometry and the distribution of elements facilitate accurate computation of flow patterns, temperature distributions, and other relevant parameters. These computational results can provide valuable insights into the performance and efficiency of the heat transfer system.

The physics of the system can be categorized into three main aspects. Firstly, the physical properties of the nanofluids, such as density, viscosity, heat capacity, and thermal conductivity, were determined based on the nanoparticle concentrations using data obtained from Figures 3-6. These properties provide important information about the behavior

of the nanofluids and their impact on heat transfer processes within the system. Secondly, the transport equations, encompassing momentum equations and energy equations, were employed to describe the conservation of mass, momentum, and energy throughout the system. These equations, as referenced from [31-33], play a crucial role in quantifying the flow patterns, pressure distributions, and temperature variations within the system. The momentum equations express the change in fluid density over time, considering the effects of fluid velocity and pressure gradients. The energy equations account for the transfer and distribution of thermal energy within the system, considering the fluid properties and temperature gradients.

The momentum equations can be expressed as:

$$\frac{\partial \rho}{\partial t} = -\nabla.(\rho U) \tag{1}$$

$$\rho\left[\frac{\partial U}{\partial t} + (U.\nabla)U\right] = \nabla\left(\mu(\nabla U + (\nabla U)^T)\right) + \rho g - \mu\beta^{-1} \tag{2}$$

$$\rho Cp\frac{\partial T}{\partial t} + \rho CpU.\nabla T = \nabla(-k\nabla T) \tag{3}$$

The absorption heat can be obtained by:

$$Qc = \rho\ q\ Cp\ \Delta T \tag{4}$$

Finally, the third aspect of the system is the implementation of boundary conditions. These boundary conditions include momentum boundary conditions for the internal pipe system, which encompass parameters such as the inlet flow rate, outlet pressures, and wall function. Additionally, heat boundary conditions are applied to the entire system, including the heat flux obtained from Figure 9 and the inlet temperature. The multiphysics nature of the system is characterized by the coupling of heat and momentum physics through convective mechanisms. The computational mesh divides the system's geometry into discrete elements, with each element containing nodes. Within each node, the algebraic equations for momentum and heat are solved using the finite element method. The solution process begins by solving the momentum equations for the entire system, and the resulting velocity fields are then used to solve the heat equation. It is important to note that the heat generated within the system affects the physical properties of both heat and momentum terms, making the solution process nonlinear. The solver must converge all the terms and configurations within the system to obtain a reliable solution.

The outcomes of the analysis include both contours analysis and parametric analysis. Contours analysis involves examining the distribution and variation of pressure and temperature within the system. In terms of temperature, the cooling duty decreases with lower flow rates, resulting in a reduced heat absorption capacity. Conversely, increasing the flow rate enhances the heat absorption capability. Consequently, higher flow rates facilitate the solar panel in approaching the desired inlet temperature of 20℃, while lower flow rates may lead to the panel operating at higher temperatures closer to 45℃.

3.2 Numerical results

The comprehensive discussion of these profiles and relationships aids in understanding the interplay between flow rates, nanoparticle concentrations, pressure drop, and heat absorption rate. This knowledge is crucial for optimizing the system's performance and ensuring efficient heat transfer within the solar-powered biodiesel reactor.

The pressure and temperature profiles depicted in Figure 9 provide valuable insights into the behavior of the system under varying intake flow rates during the month of June. The gradual decrease in pressure along the pipe from the upstream to the downstream region is primarily influenced by viscous forces. As the inlet flow rate increases, the pressure drop becomes more pronounced due to the growing dominance of momentum's inertia forces over viscous forces.

These profiles enable us to understand the system's efficiency and performance in terms of pressure distribution and temperature control. By analyzing these profiles, we can gain insights into the flow behavior and assess the effectiveness of the system in maintaining desired operating conditions. Additionally, parametric studies, along with these profiles, allow for a comprehensive evaluation of the system's performance under different operating conditions. This information is vital for optimizing the system's efficiency, enhancing its performance, and achieving the desired heat absorption rates [31].

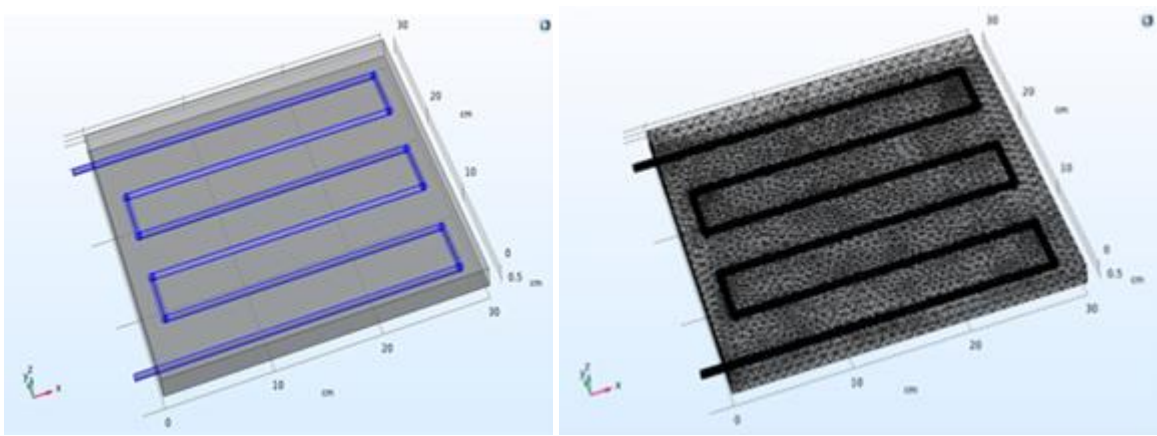

Figure 8. Geometry and mesh analysis

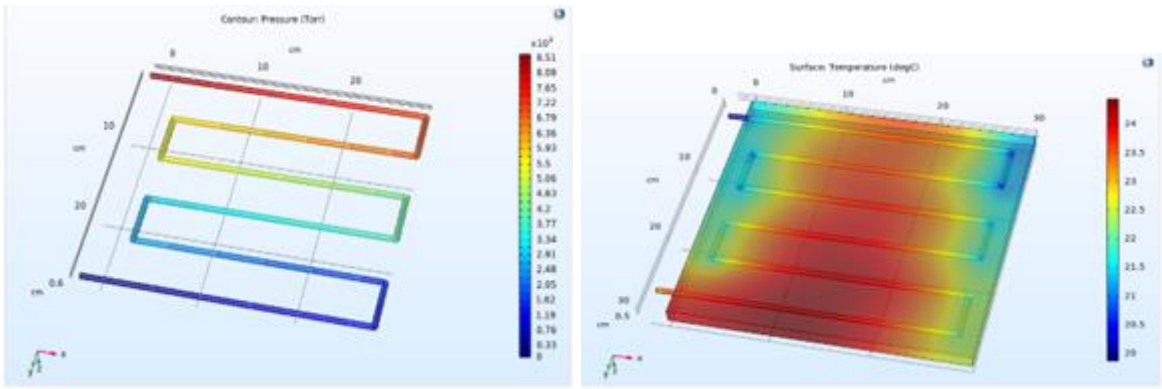

(a)

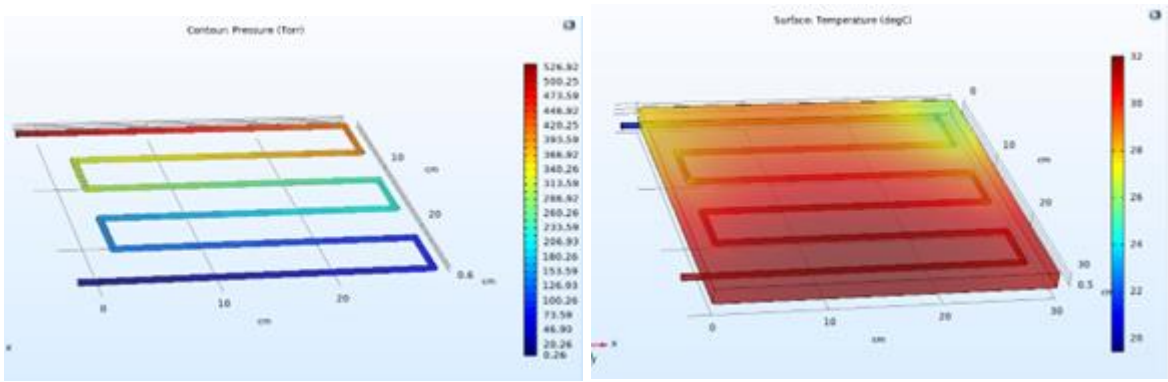

(b)

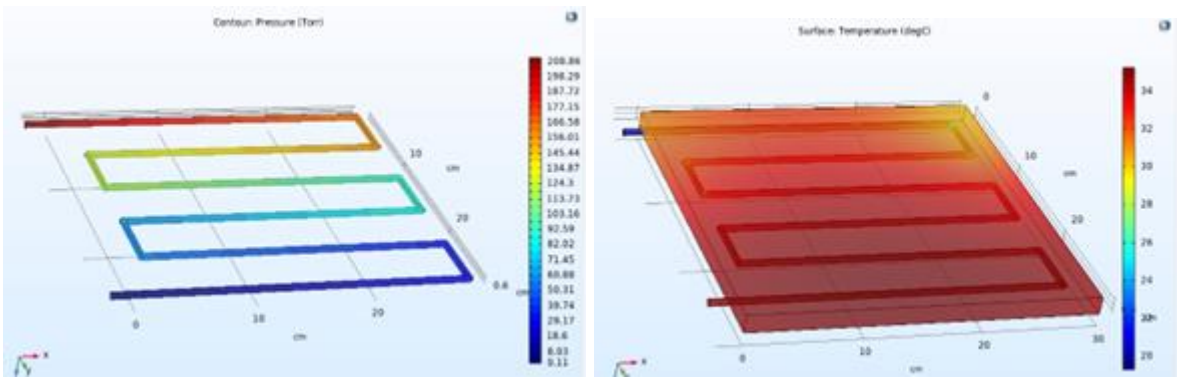

(c)

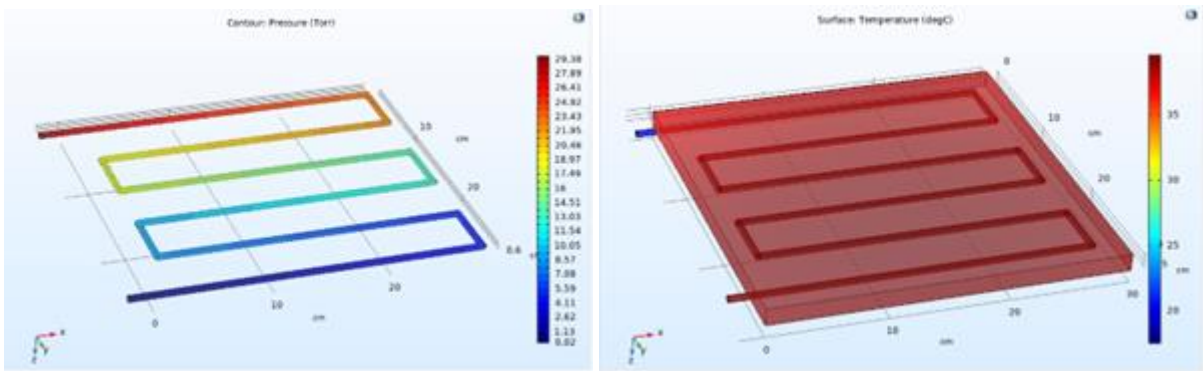

(d)

Figure 9. The contour analysis of pressure and temperature for various flow rates (q): (a) q=0.0000283 m^3/s, (b) q=0.00000283 m^3/s, (c) q=0.000001415 m^3/s, (d) q=0.000000283 m^3/s

Moving forward, Figure 10 presents the relationship between pressure drop and the nanoparticle concentration (fi) for various flow rates (q). It is observed that within the range of 0.5 to 2% nanoparticle concentration, the pressure drop does not exhibit a significant variation. This suggests that the concentration of nanoparticles in the viscous sublayer of the oil phase does not reach alarmingly high levels.

Furthermore, Figure 11 explores the relationship between

heat absorption rate (Qc) and flow rate (q) for different nanoparticle concentrations (fi). As the nanoparticle concentration increases, both the thermal conductivity and density of the nanofluid increase [32, 33]. These changes contribute to an increased heat absorption rate, as the system strives to maximize the endothermic reaction rate within the pipe.

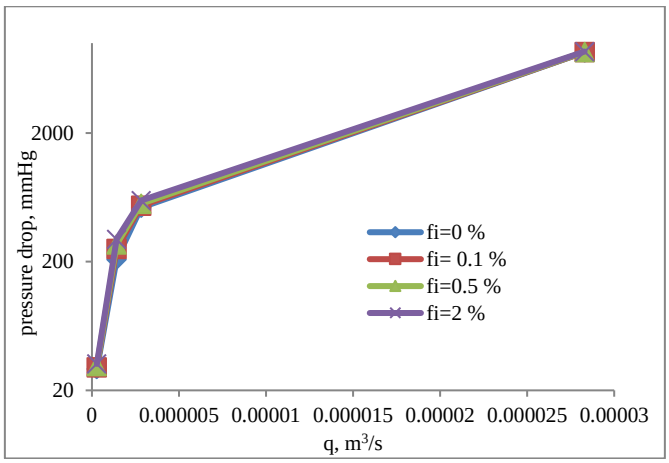

Figure 10. Pressure drop vs. q for various fi in June

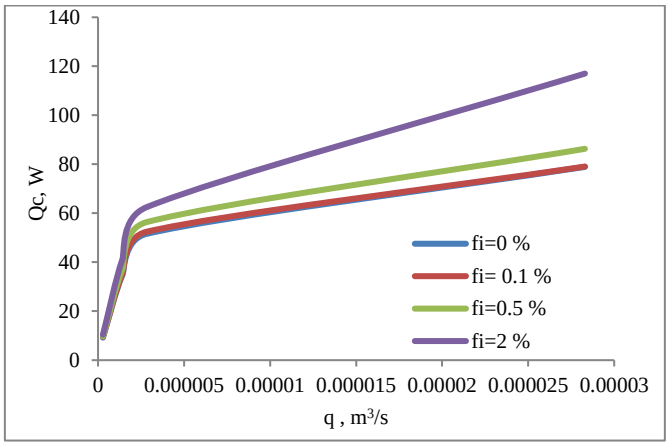

Figure 11. Qc vs. q for various fi in June

4. STATISTICAL WORK

The research procedure for utilizing MINITAB to perform regression analysis, ANOVA, Pareto chart, and surface response in a study involves several key steps. Firstly, researchers need to collect relevant data on the variables of interest and ensure the data is accurately organized and inputted into MINITAB. Following this, a regression analysis is conducted by specifying the appropriate regression model based on the research objectives and running the analysis in MINITAB to obtain the regression equation and coefficient estimates. The statistical significance of the coefficients is then assessed using t-tests or p-values. Next, an ANOVA analysis is performed in MINITAB to evaluate the overall significance of the regression model and the individual terms. The results from the ANOVA table, including sum of squares, degrees of freedom, F-values, and p-values, are interpreted to determine the significance of the model and the specific terms.

A Pareto chart is created in MINITAB to visually display and prioritize the factors based on their contributions to the response variable. The factors are ranked based on their effect sizes determined from the regression coefficients, allowing researchers to identify the most significant factors for further investigation or optimization.

Additionally, a surface response plot is generated in MINITAB to examine the relationship between the input factors and the response variable. By defining the range of values for the input factors, researchers can observe changes in the response variable and gain insights into the optimal settings for the factors and their impact on the response.

Finally, the findings from the regression analysis, ANOVA, Pareto chart, and surface response are interpreted, taking into account the research objectives. The implications of the results are discussed, including their contribution to the existing knowledge in the field. Any assumptions or limitations associated with the analysis are acknowledged, and future research directions and potential areas for further investigation are recommended.

In order to investigate the interaction between parameters and their impact on the response variable (Qc), a design of experiment tool called MINITAB was utilized. The parameters considered were nanoparticle concentration (fi) and flow rate (q), while the response variable was the heat absorption rate (Qc). The statistical analysis involved determining the significance of the parameters, surface response analysis, and optimization analysis, which are presented in Figures 12 and 13.

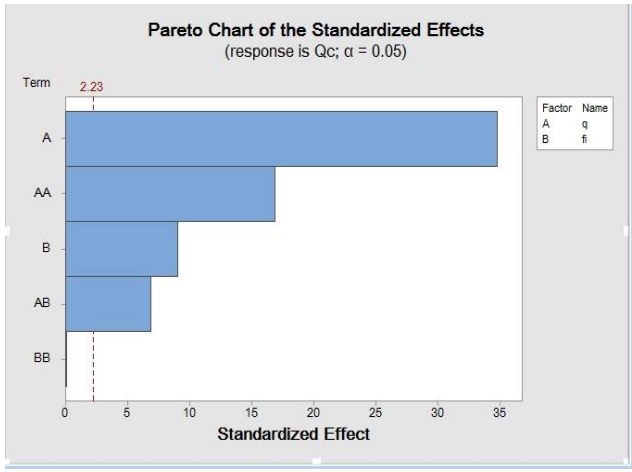

Figure 12. The interaction of significance between parameters

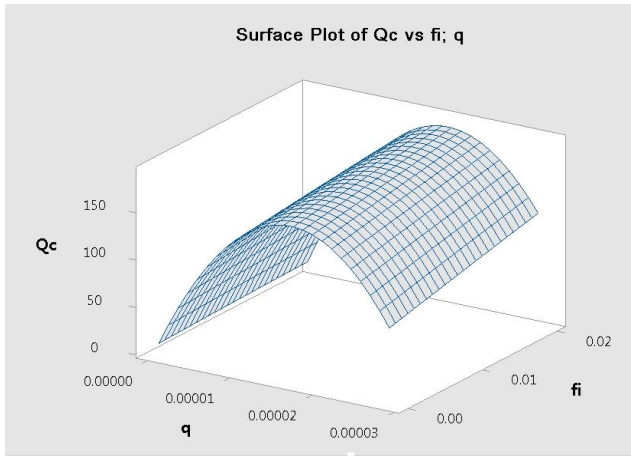

Figure 13. The surface response of present investigation

From the analysis, it was found that the flow rate (q) had the most significant influence on the heat absorption rate (Qc). The interaction between the parameters is illustrated in Figure 12, demonstrating the relationship between fi, q, and Qc. The correlation between the parameters was also examined. These results provide valuable insights into the relationship between the parameters and the response variable.

Figure 13 presents the optimal operating conditions, which are determined as a nanoparticle concentration (fi) of 2% and a flow rate (q) of 0.0000173 m^3/s. Under these optimal conditions, the heat absorption rate (Qc) was found to be 188 W. These findings highlight the importance of selecting appropriate values for the parameters to achieve optimal performance in the solar-powered biodiesel reactor.

The statistical methodology employed in this study involved regression analysis and analysis of variance (ANOVA). The regression analysis yielded a surface response equation (Eq. (5)) that represents the relationship between the parameters (fi and q) and the response variable (Qc). The R^2 value of 0.99 indicates a strong correlation between the parameters and the response variable, with a degree of confidence level greater than 99.9%. It is important to note that statistical methodologies have limitations, and the results should be interpreted within their context. The assumptions made in the design of experiments and the analysis of variance should be considered, and any potential sources of error or bias in the results should be acknowledged. Nevertheless, the statistical findings provide valuable insights into the performance of the solar-powered biodiesel reactor and contribute to the overall understanding of the system's behavior and optimization possibilities. Based on the ANOVA table, the model is found to be significant, as indicated by the low p-value of 0.001. This suggests that the regression model provides a good fit to the data.

The linear terms, including fi and q, also show significant effects on the response variable Qc, as indicated by their low p-values of 0.001. This suggests that both fi and q have a significant impact on the heat absorption rate. Furthermore, the square terms, including fi^2 and q^2, are also found to be significant, with p-values of 0.001. This indicates that the quadratic effects of both fi and q are important in explaining the variation in Qc. The error term represents the residual variation that is not explained by the model. The total sum of squares (Adj SS) captures the total variation in the response variable, and the error sum of squares (SS) measures the unexplained variation. In terms of the degrees of freedom (DF), the model has 4 degrees of freedom, indicating the number of terms included in the model. The error has 10 degrees of freedom, representing the number of observations minus the number of parameters estimated. Based on the F-values, the linear and square terms in the model are significant, indicating that they contribute significantly to the variation in Qc. The F-value is a ratio of the mean square values, representing the ratio of the explained variation to the unexplained variation. With a degree of confidence level of 0.95 (or a significance level of 0.05), the p-values in the ANOVA table indicate that all terms in the model are statistically significant, as they are below the significance level (Table 1). Therefore, we can have a high degree of confidence that the observed effects of fi and q, as well as their interaction, are not due to random chance, but are indeed significant contributors to the heat absorption rate (Qc).

$$Qc = 4.85 + 19415579\,q + 281\,fi - 595488648418\,q^2 - 3976\,fi^2 + 62606946\,q\,fi \quad (5)$$

Table 1. ANOVA analysis of present work

Source	DF	Adj SS	Adj MS	F-Value	P-Value
Model	4	60000.4	15000.1	272.7291	0.001
Linear	2	13516.6	6758.3	122.8782	0.001
fi	1	56.4	56.4	1.025455	0.001
q	1	13389.2	13389.2	243.44	0.001
Square	2	15850.6	7925.3	144.0964	0.001
fi*fi	1	0	0	0	0.001
q*q	1	12103.7	12103.7	220.0673	0.001
Error	10	44	55		
Total	14	60000.4			

5. CONCLUSIONS

The numerical examination of thermal analysis for the solar PV cell reactor in biodiesel production has been successfully conducted. The study focused on the development of a WCO-Alumina nanofluid for cooling photovoltaic cells and biodiesel, presenting a dual-function innovation approach. The computational fluid dynamics (CFD) analysis demonstrated the influence of both flow rate (q) and nanoparticle concentration (fi) on the heat absorption rate (Qc). The optimal operating conditions were identified as q=0.0000173 m^3/s and fi=2%, based on both statistical significance and economic considerations. The flow rate was found to be the most influential parameter affecting Qc.

The development of a WCO-Alumina nanofluid and its application in the cooling of photovoltaic cells and biodiesel production have significant implications for the field. The dual-function approach not only contributes to the preservation of the plumbing oil system and the reduction of emissions but also offers potential economic benefits. The study advances our understanding of the thermal behavior of solar-powered biodiesel reactors and demonstrates the effectiveness of using nanofluids for enhanced heat absorption. It contributes to the growing body of knowledge on sustainable energy systems and provides valuable insights for optimizing the performance and efficiency of solar PV cell reactors. It is important to acknowledge the limitations of the study. The findings are based on numerical simulations and experimental data obtained under specific conditions. Assumptions and simplifications were made in the model, experimental setup, and statistical analysis. Future research should focus on validating the results through additional experiments and real-world testing. Further investigations could explore the long-term stability and performance of the WCO-Alumina nanofluid, as well as evaluate its impact on the overall biodiesel production process. Additionally, studies on the economic feasibility and scalability of implementing such dual-function innovation approaches would be beneficial for practical implementation in the renewable energy industry.

REFERENCES

[1] Al-Shamani, A.N., Yazdi, M.H., Alghoul, M.A., Abed, A.M., Ruslan, M.H., Mat, S., Sopian, K. (2014). Nanofluids for improved efficiency in cooling solar collectors–A review. Renewable and Sustainable Energy Reviews, 38: 348-367. https://doi.org/10.1016/j.rser.2014.05.041

[2] Hamdan, M.A., Kardasi, K.K. (2017). Improvement of photovoltaic panel efficiency using nanofluid.

International Journal of Thermal & Environmental Engineering, 14(2): 143-151. https://doi.org/10.5383/ijtee.14.02.008

[3] Ahmed, A., Baig, H., Sundaram, S., Mallick, T.K. (2019). Use of nanofluids in solar PV/thermal systems. International Journal of Photoenergy, 2019: 8039129. https://doi.org/10.1155/2019/8039129

[4] Malvi, C.S., Dixon-Hardy, D.W., Crook, R. (2011). Energy balance model of combined photovoltaic solar-thermal system incorporating phase change material. Solar Energy, 85(7): 1440-1446. https://doi.org/10.1016/j.solener.2011.03.027

[5] Su, D., Jia, Y., Lin, Y., Fang, G. (2017). Maximizing the energy output of a photovoltaic–thermal solar collector incorporating phase change materials. Energy and Buildings, 153: 382-391. https://doi.org/10.1016/j.enbuild.2017.08.027

[6] Ahmed, O.K., Mohammed, Z.A. (2017). Influence of porous media on the performance of hybrid PV/Thermal collector. Renewable Energy, 112: 378-387. https://doi.org/10.1016/j.renene.2017.05.061

[7] Alva, G., Liu, L., Huang, X., Fang, G. (2017). Thermal energy storage materials and systems for solar energy applications. Renewable and Sustainable Energy Reviews, 68: 693-706. https://doi.org/10.1016/j.rser.2016.10.021

[8] Herrando, M., Markides, C.N., Hellgardt, K. (2014). A UK-based assessment of hybrid PV and solar-thermal systems for domestic heating and power: System performance. Applied Energy, 122: 288-309. https://doi.org/10.1016/j.apenergy.2014.01.061

[9] Kumar, R., Deshmukh, V., Bharj, R.S. (2020). Performance enhancement of photovoltaic modules by nanofluid cooling: A comprehensive review. International Journal of Energy Research, 44(8): 6149-6169. https://doi.org/10.1002/er.5285

[10] Albadr, J., Tayal, S., Alasadi, M. (2013). Heat transfer through heat exchanger using Al_2O_3 nanofluid at different concentrations. Case Studies in Thermal Engineering, 1(1): 38-44. https://doi.org/10.1016/j.csite.2013.08.004

[11] Xuan, Y., Li, Q. (2000). Heat transfer enhancement of nanofluids. International Journal of Heat and Fluid Flow, 21(1): 58-64. https://doi.org/10.1016/S0142-727X(99)00067-3

[12] Senthilraja, S., Vijayakumar, K.C.K. (2013). Analysis of heat transfer coefficient of CuO/water nanofluid using double pipe heat exchanger. International Journal of Engineering Research and Technology, 6(5): 675-680.

[13] Gupta, N.K., Tiwari, A.K., Ghosh, S.K. (2018). Heat transfer mechanisms in heat pipes using nanofluids–A review. Experimental Thermal and Fluid Science, 90: 84-100. https://doi.org/10.1016/j.expthermflusci.2017.08.013

[14] Mangrulkar, C.K., Kriplani, V.M., Dhoble, A.S. (2016). Experimental investigation of convective heat transfer enhancement using alumina/water and copper oxide/water nanofluids. Thermal Science, 20(5): 1681-1692. https://doi.org/10.2298/TSCI141225077M

[15] Buongiorno, J., Hu, L.W. (2009). Nanofluid heat transfer enhancement for nuclear reactor applications. In International Conference on Micro/Nanoscale Heat Transfer, 43918: 517-522. https://doi.org/10.1115/MNHMT2009-18062

[16] Sekhar, Y.R., Sharma, K.V., Karupparaj, R.T., Chiranjeevi, C. (2013). Heat transfer enhancement with Al_2O_3 nanofluids and twisted tapes in a pipe for solar thermal applications. Procedia Engineering, 64: 1474-1484. https://doi.org/10.1016/j.proeng.2013.09.229

[17] Bianco, V., Manca, O., Nardini, S., Vafai, K. (2015). Heat transfer enhancement with nanofluids. CRC Press. https://books.google.com.my/books?id=v5S9BwAAQBAJ.

[18] Mohsen, O.A., Muhammed, M.A., Hasan, B.O. (2021). Heat transfer enhancement in a double pipe heat exchanger using different fin geometries in turbulent flow. Iranian Journal of Science and Technology, Transactions of Mechanical Engineering, 45: 461-471. https://doi.org/10.1007/s40997-020-00377-2

[19] Khaled, A.R., Vafai, K. (2005). Heat transfer enhancement through control of thermal dispersion effects. International Journal of Heat and Mass Transfer, 48(11): 2172-2185. https://doi.org/10.1016/j.ijheatmasstransfer.2004.12.035

[20] Sivashanmugam, P. (2012). Application of nanofluids in heat transfer. An Overview of Heat Transfer Phenomena, 16: 411-441. https://doi.org/10.5772/2623

[21] Borate, K.S., Gawandare, A.V., Kapatkar, P.V.N. (2016). Heat transfer enhancement with different square jagged twisted tapes and Cuo/water nano fluid. International Journal on Theoretical and Applied Research in Mechanical Engineering, 4(2): 31-35.

[22] Zamzamian, A., Oskouie, S.N., Doosthoseini, A., Joneidi, A., Pazouki, M. (2011). Experimental investigation of forced convective heat transfer coefficient in nanofluids of Al_2O_3/EG and CuO/EG in a double pipe and plate heat exchangers under turbulent flow. Experimental Thermal and Fluid Science, 35(3): 495-502. https://doi.org/10.1016/j.expthermflusci.2010.11.013

[23] Hussein, A.M., Bakar, R.A., Kadirgama, K. (2014). Study of forced convection nanofluid heat transfer in the automotive cooling system. Case Studies in Thermal Engineering, 2: 50-61. https://doi.org/10.1016/j.csite.2013.12.001

[24] Liu, M., Lin, M. C., Wang, C. (2011). Enhancements of thermal conductivities with Cu, CuO, and carbon nanotube nanofluids and application of MWNT/water nanofluid on a water chiller system. Nanoscale Research Letters, 6: 1-13. https://doi.org/10.1186/1556-276X-6-297

[25] Majdi, H.S., Alabdly, H.A., Hamad, M.F., Hasan, B.O., Hathal, M.M. (2019). Enhancement of heat transfer using aluminum oxide nanofluid on smooth and finned surfaces with COMSOL multiphysics simulation in turbulent flow. Al-Nahrain Journal for Engineering Sciences, 22(1): 44-54.

[26] Sundar, L.S., Singh, M.K. (2013). Convective heat transfer and friction factor correlations of nanofluid in a tube and with inserts: A review. Renewable and Sustainable Energy Reviews, 20: 23-35. https://doi.org/10.1016/j.rser.2012.11.041

[27] Phan, A.N., Phan, T.M. (2008). Biodiesel production from waste cooking oils. Fuel, 87(17-18): 3490-3496. https://doi.org/10.1016/j.fuel.2008.07.008

[28] Degfie, T.A., Mamo, T.T., Mekonnen, Y.S. (2019). Optimized biodiesel production from waste cooking oil (WCO) using calcium oxide (CaO) nano-catalyst.

Scientific Reports, 9(1): 18982. https://doi.org/10.1038/s41598-019-55403-4
[29] Sadaf, S., Iqbal, J., Ullah, I., Bhatti, H.N., Nouren, S., Nisar, J., Iqbal, M. (2018). Biodiesel production from waste cooking oil: An efficient technique to convert waste into biodiesel. Sustainable Cities and Society, 41: 220-226. https://doi.org/10.1016/j.scs.2018.05.037
[30] Zhang, J.Z., Li, J., Li, Y., Zhao, Y. (2014). Hydrogen Generation, Storage and Utilization. John Wiley & Sons. https://doi.org/10.1002/ejoc.201200111
[31] Hathal, M.M., Hasan, B.O., Majdi, H.S. (2023). The impact of gas-liquid dispersed flow on heat exchanger performance with improvement using CuO nanofluid. Engineering Innovations, 6: 1-22. https://doi.org/10.4028/p-gdl41l
[32] Hathal, M.M., Hasan, B.O. (2020). Studying the effect of operating parameters on the removal of nickel ion from an adsorber by using COMSOL multiphysics simulation. Al-Nahrain Journal for Engineering Sciences, 23(4): 357-364. https://doi.org/10.29194/njes.23040357
[33] Majdi, H.S., Alabdly, H.A., Hamad, M.F., Hasan, B.O., Hathal, M.M. (2019). Enhancement of heat transfer using aluminum oxide nanofluid on smooth and finned surfaces with COMSOL multiphysics simulation in turbulent flow. Al-Nahrain Journal for Engineering Sciences, 22(1): 44-54.

NOMENCLATURE

T	Temperature, ℃
U	Fluid velocity, m/s
q	Inlet flow rate, m^3/s
K	Thermal conductivity, W/m. ℃
Cp	Heat capacity J/kg., ℃
g	Gravity acceleration, m/s^2
Qc	Absorption heat, W

Greek letters

ρ	Density, Kg/m^3
μ	viscosity, Pa.s